International Journal of Nanomedicine

Dovepress
open access to scientific and medical research

Open Access Full Text Article

ORIGINAL RESEARCH

# Nobiletin-loaded micelles reduce ovariectomy-induced bone loss by suppressing osteoclastogenesis

This article was published in the following Dove Press journal:
*International Journal of Nanomedicine*

Yabing Wang[1]
Jian Xie[1]
Zexin Ai[2]
Jiansheng Su[1]

[1]Department of Prosthodontics, School & Hospital of Stomatology, Tongji University, Shanghai Engineering Research Center of Tooth Restoration and Regeneration, Shanghai 200072, People's Republic of China; [2]Department of Oral and Maxillofacial Surgery, School and Hospital of Stomatology, Tongji University, Shanghai Engineering Research Center of Tooth Restoration and Regeneration, Shanghai 200072, People's Republic of China



**Background:** Nobiletin (NOB), a polymethoxy flavonoid, possesses anti-cancer and anti-inflammatory activities, has been reported that it played role in anti-osteoporosis treatment. However, previous research did not focus on practical use due to lack of hydrophilicity and cytotoxicity at high concentrations. The aim of this study was to develop a therapeutic formulation for osteoporosis based on the utilization of NOB.

**Methods:** In this study, NOB-loaded poly(ethylene glycol)-block-poly(e-caprolactone) (NOB-PEG-PCL) was prepared by dialysis method. The effects on osteoclasts and anti-osteoporosis functions were investigated in a RANKL-induced cell model and ovariectomized (OVX) mice.

**Results:** Dynamic light scattering and transmission electron microscopy examination results revealed that the NOB-PEG-PCL had a round shape, with a mean diameter around 124 nm. The encapsulation efficiency and drug loading were 76.34±3.25% and 7.60±0.48%, respectively. The in vitro release of NOB from NOB-PEG-PCL showed a remarkably sustained releasing characteristic and could be retained at least 48 hrs in pH 7.4 PBS. Anti-osteoclasts effects demonstrated that the NOB-PEG-PCL significantly inhibited the formation of tartrate-resistant acid phosphatase (TRAP)-positive multinuclear cells stimulated by RANKL. Furthermore, the NOB-PEG-PCL did not produce cytotoxicity on bone marrow-derived macrophages (BMMs). The mRNA expressions of genetic markers of osteoclasts including TRAP and cathepsin K were significantly decreased in the presence of NOB-PEG-PCL. In addition, the NOB-PEG-PCL inhibited OC differentiation of BMMs through RANKL-induced MAPK signal pathway. After administration of the NOB-PEG-PCL, NOB-PEG-PCL prevented bone loss and improved bone density in OVX mice. These findings suggest that NOB-PEG-PCL might have great potential in the treatment of osteoporosis.

**Conclusion:** The results suggested that NOB-PEG-PCL micelles could effectively prevent NOB fast release from micelles and extend circulation time. The NOB-PEG-PCL delivery system may be a promising way to prevent and treat osteoporosis.

**Keywords:** nobiletin, micelles, TRAP, ovariectomized (OVX) mice

Correspondence: Jiansheng Su
Department of Prosthodontics, School & Hospital of Stomatology, Tongji University, Shanghai Engineering Research Center of Tooth Restoration and Regeneration, Shanghai 200072, People's Republic of China
Tel +86 215 672 2215
Fax +86 216 652 4025
Email sjs@tongji.edu.cn

## Introduction

Bone balanced via the combination of bone resorption and bone formation is a dynamic tissue.[1,2] Osteoporosis is a common, potentially severe bone disease due to decrease in ovarian estrogen and an increase in bone resorption and therefore produces severe physical disabilities to the patients, mainly for postmenopausal women.[3,4] It is known that estrogen can decrease osteoclastogenesis.[5] Estrogen

deficiency stimulates cortical porosity and therefore forming resorption areas on the trabecular surface.[6,7] It has been recently demonstrated that osteoporosis treatment exploits on improving bone regeneration or inhibiting bone resorption.[8,9]

At the cellular level, interaction and communication between the main bone-cell types, the bone-forming osteoblasts and the bone-degrading osteoclasts, organize the smallest functional unit on bone metabolism including osteogenesis which is reduced/ineffective in osteoporotic bone and the important effect of osteoclastogenesis activation. Bone resorption is regulated by osteoclasts (OC).[10] Osteoclasts are originated from hematopoietic cells belonging to monocyte/macrophage lineage.[11] Osteoclasts have some similar characteristics with macrophages such as morphological and functional features.[12,13] Osteoclasts are important to maintain healthy bones so that negative effects could be observed during anti-osteoporotic treatment based on RANK-pathway inactivation. Macrophage-colony-stimulating factor (M-CSF) and receptor activator of nuclear factor-κB ligand (RANKL) are two important molecules necessary for osteoclastogenesis.[14,15] When the RANKL combines with its receptor which is RANK, they provoke signaling pathways for inducing OC differentiation including the producing of reactive oxygen species (ROS) and nuclear factor in activated T-cells, cytoplasmic 1 (NFAT1).[16,17] Further, the expression of calcitonin receptor and tartrate-resistant alkaline phosphatase (TRAP) are caused by activated transcription factors.[18]

Denosumab was the first RANKL inhibitor approved by the Europe and the US for the treatment of osteoporosis. At first, denosumab was designed to antagonize RANKL by recombinant OPG protein; however, it was found that denosumab can neutralize antibodies against OPG. Furthermore, denosumab and romosozumab as antibodies will face challenges because of the structural complexity and large molecular size of these proteins.[19] However, nobiletin (NOB), a polymethoxyflavone abundantly in oranges peel, has been reported to exhibit several biological activities with simple structural and small molecular size.[20,21] Previous studies have shown that nobiletin has an anti-tumor promoting influence on diverse kinds of cancer cells and inhibits inflammatory pathways.[22,23] One of the molecular mechanisms could be regulation of RANKL-induced osteoclastogenesis. It has been reported that Nobiletin not only can obviously inhibit bone resorption but repair the lower bone density in ovariectomized (OVX) mice imitating the situation of postmenopausal osteoporosis.[24]

The major benefits of drug delivery system compared with actual clinical evaluated drugs are the enhancement of the bioavailability of various active molecules. Some active molecules are easily inactivated by light or enzymatic attack, but the use of carriers as drug delivery systems can protect drug from inactivation and reduce its toxicity.[25] The use of carriers as drug delivery systems also avoids unlikable taste of some drugs. Drug delivery systems can achieve more biodistribution of the active molecule by no longer its own physicochemical properties but on carrier's ones.[26] As we know, drug solutions are often unfavorable long-term administration because of poor solubility and low bioavailability, which result in unrealistic administration system for clinical practice.[27,28] Moreover, the use of carriers as drug delivery systems can provide better membrane absorption and can target more drugs to the tissue compared to drug solutions.[29]

Polymeric biomaterials have been reported that they could be used to overcome multiple drug resistance in cancer and multifunctional approaches could utilize polymeric micelles to circumvent multidrug-resistant tumors.[30,31] Polymeric biomaterials as a promising approach in bone tissue engineering (BTE) have been identified and propelled in recent years.[32] It is known that they have many properties such as excellent bio-compatibility, controlled biodegradability and good mechanical strength. But these biomaterials such as polycaprolactone (PCL), polylactide (PLA), Polyhydroxyalkanoate (PHA), poly(gly-colic acid) (PGA) have disadvantages because of their hydrophobic nature. Therefore, a hydrophilic poly(ethylene glycol) (PEG) can be used as an amphiphilic polymeric system within polymeric biomaterials. The amphiphilic micelles shaped in aqueous condition including a core-shell structure stock insolubility drugs by the hydrophobic core and keep a stable structure in an aqueous condition through the hydrophilic group.[33] Furthermore, the micellar delivery system may provide more drug accumulated in bone tissues due to its nanosize effect.[34] Therefore, it represents a more effective and safe treatment compared to repeated local injections. Moreover, it was first reported that polymeric biomaterials combined with NOB and it made a suitable candidate for BTE.

Therefore, it is necessary to develop effective and new methods. Micellar delivery system has also more benefits: (1) sustained circulation period; (2) amplified accumulation; (3) defense from degradation by enzyme. Hence, we

investigate mPEG-PCL micelles that encapsulate hydrophobic nobiletin for the treatment of osteoporosis. We also study diverse properties of micelles including micellar characteristics, cytotoxicity, pharmacokinetic behaviors, therapeutic effects of nobiletin-loaded PEG-PCL (NOB-PEG-PCL) micelles in ovariectomy-induced osteoporosis mode through their action on osteoclastogenesis.

# Materials and methods

## Materials

Tangerine was obtained from the Bozhou medicinal material market (Anhui, China); Poly (ethylene glycol)2000-block-poly(e-caprolactone)2000 (mPEG-PCL) were purchased from Jinan DaiGang Biomaterials Company (Shangdong, China). Antibodies were obtained from Cell Signaling Technology Inc (Beverly, MA) to anti-phospho-ERK1/2 (42/44 kDa) and anti-ERK1/2 (42/44 kDa). Antibodies were obtained from Cell Signaling Technology Inc to anti-phospho-p38 MAPK (42 kDa), anti-p38 MAPK (42 kDa). Antibodies were obtained from Cell Signaling Technology Inc to anti-active JNK1/2 (46/54 kDa) and anti-JNK1/2 (46/54 kDa). CCK-8 was purchased from Dojindo (Kumamoto, Japan) to assess cell proliferation. Dulbecco's modified Eagle's medium (DMEM) (Life Technologies, Australia, 10568024) and Dimethyl sulfoxide (DMSO) were from Sigma-Aldrich (St. Louis, USA). Fetal bovine serum (FBS) was purchased from Gibco (Life Technologies, Australia, 10099-141/1414426). All other solvents and reagents were of chemical grade.

## Preparation of nobiletin

The dried peel of Tangerine was chopped to powder and separated by 80% ethanol for three times. The extraction interval was set at 2, 2 and 1 hr, respectively. Then the extract was filtrated, combined and evaporated to dryness at 45°C under reduced pressure by rotary vaporization. By stepwise eluting on D101 microporous resin, the water-soluble extract was chromatographed. Target sample was yield by 80% ethanol. Then 20 g of crude sample was obtained. With a solvent system composed of *n*-hexane–ethyl acetate–methanol–water (1:0.8:1:1, v/v), this sample was detached by high-speed counter-current chromatography (HSCCC). Then, the structure of nobiletin was determined by proton and carbon-13 nuclear magnetic resonance spectra. The purity of nobiletin (99.2%) was measured by high-performance liquid chromatography (Figure 1A).

## Synthesis of NOB-PEG-PCL

Micelles containing Nobiletin were prepared as follows. 100 mg of PEG-b-PCL and Nobiletin (10 mg) were firstly

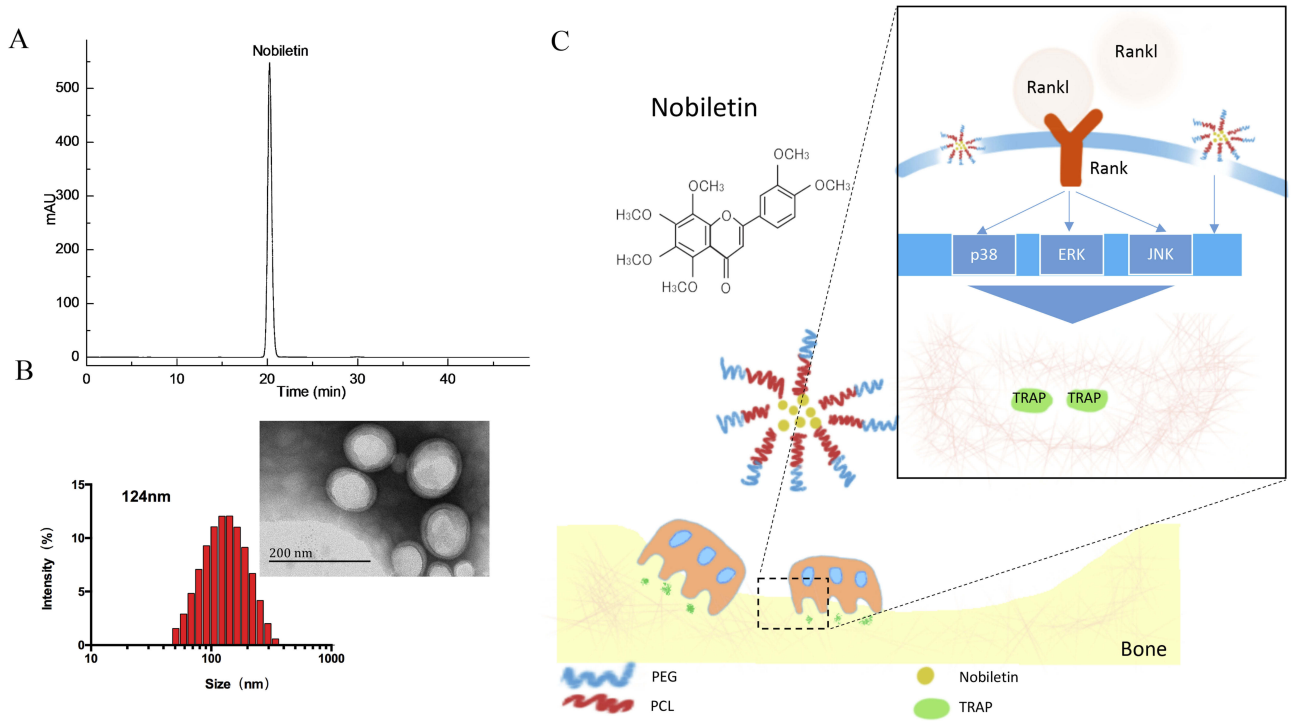


**Figure 1** (**A**) HPLC chromatogram of NOB. (**B**) The diameter distributions of NOB-loaded micelles. The insert picture is the TEM image of NOB-loaded micelles. Scale bar =200 nm. (**C**) Schematic illustrations of the effect of the NOB-loaded micelles on osteoclasts via MAPKs process stimulated by RANKL.

dissolved in DMSO. Deionized water was dropped into the above suspension by continuously stirring. Then Spectra/Por membrane MWCO:8000 was used to dialyze the suspension and deionized water was changed at least eight times. The obtained nanoparticles were collected by 13-mm syringe filter (0.2 μm, millipore). Water-insoluble byproducts were removed by centrifugation at 12,000 rpm and then the dialyzed solution was freeze-dried to achieve NOB-PEG-PCL.

## Characterization of NOB-PEG-PCL

A Nano-Zs Malvern Nano analyzer was used to detect the determination of particle size. The date of particle size was averaged from five measurements. When a drop of PEG-b-PCL micelle solution was air-dried at framework treated with carbon film and formvar, an H-600 Transmission electron microscope (TEM) could be used to observe micelle morphology. Accelerating voltage of 65 kV was used to obtain the TEM images.

To measure the content of NOB, an ultraviolet-visible spectrophotometer (Optizen 3220; Mecasys, Daejeon, Korea) was used to determine the drug loading and encapsulation by suspending frozen and dried micelles into DMSO. In order to obtain a well-proportioned solution, the suspension was placed in an Elmasonic P30 H ultrasonic bath (ultrasound frequency of 80 kHz and power of 130 W) for 2 hrs. Different concentrations of NOB (0.01–50 μg) versus maximum absorbance were observed to form a standard calibration curve at the highest-spectrum wavelengths (290 nm). To confirm reproducibility, all data were tested in triplicate. Eqs. (1) and (2) were used to determine the encapsulation efficiency (EE) and loading capacity (LC).

$$EE(\%) = \left(\frac{\text{Amount of loaded drug}}{\text{Amount of feeding drug}}\right) \times 100 \quad (1)$$

$$LC(\%) = \left(\frac{\text{Amount of loaded drug}}{\text{Amount of drug} - \text{loaded micelle}}\right) \times 100\% \quad (2)$$

## In vitro drug release

The dialysis method was used to investigate the release performance of NOB-PEG-PCL micelles. Flat dialysis membranes (MWCO, 7.0 kDa) 32-mm wide (Spectra/Por® Dialysis Membrane Products) were used. The membranes were boiled for 30 mins in 40% ethanol, soaked in 1 mM ethylenediamine tetraacetic acid (EDTA; BDH Ltd., Poole, UK) for 30 mins, rinsed several times with Milli-Q water, stored in 0.01 M $NaHCO_3$ and rinsed with Milli-Q water before use. The dialysis bag loaded 50 mL Phosphate Buffered Saline (PBS) (pH, 7.4) with free NOB and NOB-PEG-PCL micelles into the bag. All data were accomplished at 37°C and in 60 rpm horizontal shaking. When 1 mL released vehicle was collected from the dialysis bag, another 1 mL PBS would be supplied into the bag at pre-set-intervals. The content of NOB was measured using UV spectroscopy at optical wavelengths of 290 nm. All drug-release tests were repeated thrice.

## Cell culture

Bone-marrow-derived macrophages (BMMs) were primarily cultured for studying OC differentiation and cell cytotoxicity. Bone-marrow-derived osteoclasts were generated by isolating 6-week mice as described.[35] At first, 30 ng/mL M-CSF was used to stimulate cells in a 10% Fetal Bovine Serum (FBS) and 1% Penicillin and Streptomycin (PS) (all these chemicals are manufactured by FUJIFILM Wako Pure Chemical Corporation ®, Osaka, Japan) medium with a wet 5% $CO_2$ environment. After this stage, cells can be considered as preosteoclasts because of the effect of 30 ng/mL M-CSF in a 10% FBS and 1% PS medium with a wet 5% $CO_2$ environment. Then, cells were treated with RANKL (100 ng/mL) and M-CSF (30 ng/mL) (R&D Systems, Inc., Minneapolis, MN, USA) to achieve OC. For studying OC, cells treated by different test supplements such as NOB, PEG-PCL, and NOB-PEG-PCL micelle and the fresh culture medium were added every 3 days.

## Cytotoxicity study

For in vitro biological evaluation, cells were cultured in well plates (Corning Incorporated, Corning, NY, USA) after centrifugation for 5 mins at 1000 rpm. The CCK-8 method was used to assay the cytotoxicity of NOB-PEG-PCL. The cells were cultured at a density of $10^4$ cells/$cm^2$ in a 96-well plate for 24 hrs and then treated with NOB 1, 5, 10, 20, 50 μM and NOB-PEG-PCL micelle (dose: containing NOB 1, 5, 10, 20, 50 μM), respectively, for 48 hrs. Each well was added CCK-8 solution for 3 hrs at the set time points and detected at 450 nm of the optical density (OD) by a spectrophotometer. Each test was repeated thrice. Untreated BMMs were set as control.

## Quantitative real-time polymerase chain reaction (real-time PCR)

BMMs were treated with RANKL (100 ng/mL) and M-CSF (30 ng/mL) to achieve OC for 5 days. For studying

osteoclastogenesis expression, cells treated by different test supplements such as NOB, PEG-PCL, and NOB-PEG-PCL micelle and the fresh culture medium were added every 3 days. According to the manufacturer's protocol, quantitative real-time PCR was used to detect osteoclastogenesis expression. Consistent with manufacturer's instructions, a RNeasy Plus Mini Kit was used to measure complete RNA of the BMMs gathered from a 48 well-culture plate. A cDNA Synthesis kit was used to produce First-strand complementary DNA (cDNA). The reverse transcription conditions were controlled at 45°C lasting 60 mins and at 95°C for 5 mins. The primers of the measured mRNA genes were as follows: the primer sequences used were: 5′-gaccaccttg gcaatgtctctg-3′ and 5′-tggctgaggaagtcatctgagttg-3′ (TRAP); 5′-tgaggcttctcttggtgtccatac-3′ and 5′aaagggtgtcattactgcggg-3′ (cathepsin K); 5′-acccagaagactgtggatgg-3′ and 5′-cacattg .ggggtaggaacac-3′ (GAPDH).

## Western blotting

When BMMs were grown to confluence, the medium including NOB, PEG-PCL, and NOB-PEG-PCL micelle was added into the cell plates and then cells were stimulated by RANKL (100 ng/mL) for 30 mins. Protein concentration was detected by loading 40 μg protein on sodium dodecylsulfate-polyacrylamide gel electrophoresis (SDS-PAGE) and then transferred to polyvinylidene fluoride membranes. After blocking overnight at 4°C in Block Ace (Dainippon Pharmaceutical, Osaka, Japan), the membranes were incubated with the phospho-ERK1/2 (Thr202/Tyr204), ERK, phospho-p38 MAPK (Thr180/Tyr182), p38 MAPK, phospho-JNK1/2 (Thr183/Tyr185), and JNK1/2. The internal control protein was $\beta$-actin. After anti-rabbit IgG or anti-goat IgG antibody was incubated with membranes, digital images were achieved by a digital gel documentation system.

## Tartrate-resistant acid phosphatase (TRAP) assay

When BMMs were grown to confluence, the medium including NOB, PEG-PCL, and NOB-PEG-PCL micelle was added into the cell plates and then cells were stimulated by RANKL (100 ng/mL) for 5 days. The medium was changed every other day. After PBS washed cells three times, a TRAP staining kit from Cell Garage was used to detect TRAP-positive cells with multinuclear containing three or more nuclei.

## Animal test

Forty C57Bl/6 mice matured 8 weeks with an average of 20 g were chosen for the study. All the animal experiments were performed in accordance with the guidelines and regulations for the care and use of laboratory animals of the National Institutes of Health. Institutional Animal Care and Use Committee of Tongji university approved the animal procedures. The experiment groups contained five groups including Sham group; OVX group; OVX group treated with NOB; OVX group treated with PEG-PCL micelles; and OVX group treated with NOB-PEG-PCL micelles, respectively. Animals in the OVX group were ovariectomized bilaterally, whereas the sham group mice were sham-operated. The OVX mice were injected intraperitoneally with NOB (dose: 50 μM) and PEG-PCL, NOB-PEG-PCL (dose: containing NOB 50 μM). After 9-week treatment, microcomputed tomography (micro-CT) system (Scanco Medical, Zurich, Switzerland) was used to detect the impact of region of interest (ROI) in the trabecular bone by quantifying the mean gray value and standard deviation. The microstructural indices of the distal femurs including bone volume/tissue volume (BV/TV), trabecular space (Tb.Sp), and bone mineral density (BMD) were calculated by using an auxiliary histomorphometric software. Following micro-CT analysis, femur samples were removed, decalcified, embedded in paraffin, and stained with hematoxylin and eosin (H&E) for histological analysis in accordance with the manufacturer's instructions (Beyotime, Shanghai, China).

## Statistical analysis

Data were expressed as the mean ± standard deviation. All experiments were performed independently in triplicate. Statistical analysis was performed using ANOVA and a Dunnett's Multiple Comparison Test. The statistical significance was controlled as $p<0.05$.

# Results and discussion

## Preparation and characterization of NOB-PEG-PCL micelles

NOB-PEG-PCL micelles could self-accumulate into polymeric vehicle in aqueous phase solution. NOB was stored by PCL which could be used to increase the drug solubility and store hydrophobic drugs. Benefiting from hydrophilic, nontoxic, the PEG chains can prolong the systemic cycling time of drug delivery systems. Furthermore, PCL block is a good material as a useful drug delivery system via

hydrophobic vehicle. Both PEG and PCL as drug carrier could decrease low toxicity and immunogenicity. PEG-PCL micelles could increase the solubility of hydrophobic drugs and therefore have been widely used as drug delivery vehicle. This strategy is well designed for efficient intracellular uptake and delivery of NOB. The UV absorption of NOB was 290 nm. The encapsulating efficiency of NOB was 76.34±3.25% and loading efficiency was 7.60±0.48%. The morphology of micelles was identified by DLS and TEM. Figure 1B exhibits that the size of NOB-PEG-PCL was 124 nm. The insert picture of Figure 1B shows that NOB-PEG-PCL micelles had a similar spherical shape which is smaller than the DLS result because of the diverse situations where DLS detect the micelle size in hydro-dynamic environment while TEM observe the dry condition. The synthesized NOB-PEG-PCL could form self-assembling micelles into a core-shell structure in aqueous medium with two important characteristics. PEG as a hydrophilic shell had good capacity to improve micellar stability in the process of self-assembling and PCL could improve drug solubility.[36] They have large development potential as drug carrier to load NOB in the bone tissue engineering (Figure 1C).

## In vitro drug release study

Figure 2 shows that the release behavior of NOB-PEG-PCL was studied in vitro by dialysis method in phosphate-buffered saline (PBS, pH 7.4). It is obviously observed that the free NOB is liberated up to 90% within 12 hrs while NOB can have prolonged release from PEG-PCL micelles more than 48 hrs. However, a typical biphasic-release profile was observed in NOB-PEG-PCL group. At first stage was an initial rapid release (0–12 hrs) and then another release stage was a prolonged time of up to 12–48 hrs. Approximately, 65% of the NOB was released from the polymeric micelles in first 12 hrs and then the remaining drug reached almost 80% during the late final time intervals (12–48 hrs). When the micelles were self-assembling, some of the NOB was concentrated on the surface of micelles. And the rest of hydrophobic drug molecules can be gradually released from the polymeric micelle core and therefore leading to a sustained release. The two-stage release mode can carry NOB to the bone, allowing enough drug concentration to the sites. Furthermore, the amount of drug intake can be reduced by micelles strategy and therefore reducing patient trouble in the future. Jun et al studied the release profile of 5-Fluorouracil (5-FU) from MPEG-b-PLA micelles.[37] The result showed that at the initial stage free 5-FU release performed a burst release (more than 72%) but there was only about 22.3% initial burst release from the 5-FU-loaded micelles. Yao et al reported the release profiles of minocycline solution and Minocycline-loaded MPEG-b-PLA micelles (MIN-PEG-b-PLA) in PBS.[38] Minocycline showed that almost 100% of the minocycline solution was released within 24 hrs; however, the cumulative release of MIN from the MIN-PEG-b-PLA was over 14 days. Therefore, the use of micelles strategy can avoid the burst release of drug to decrease the amount of drug intake.

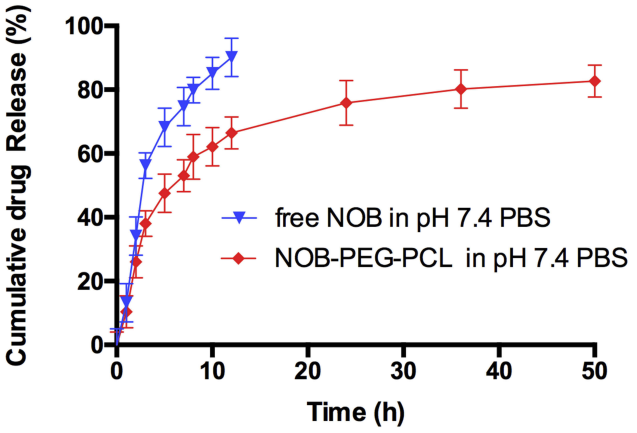


**Figure 2** In vitro release of free NOB and NOB-loaded micelles in pH 7.4 PBS (mean ± SD).

## Cytotoxicity

The BMMs viability at different concentrations of NOB, NOB-PEG-PCL was detected by CCK-8 assay (Figure 3). NOB at 50 μM concentrations was toxic for BMMs and NOB showed no cytotoxic results up to 20 μM (Figure 3A). PEG-PCL and NOB-PEG-PCL showed no obvious cell cytotoxicity treated with different concentrations even at the highest concentration tested (1, 5, 10, 20, 50 μM) (Figure 3B). It was reported previously that PEG-PCL did not trigger damage to internal organs; however, it may cause accumulation in organs after intraperitoneal injection.[39] In this work, it showed that NOB-PEG-PCL system was cytocompatible unlike NOB alone which was cytotoxic at high concentrations and therefore was important for drug delivery.

## Effects on OC formation

For investigating the influence of NOB-PEG-PCL on osteoporosis, we assess the inhibition of NOB-PEG-PCL on OC formation from BMM. Figure 4A shows that NOB (dose: 50 μM) and NOB-PEG-PCL (dose: containing NOB

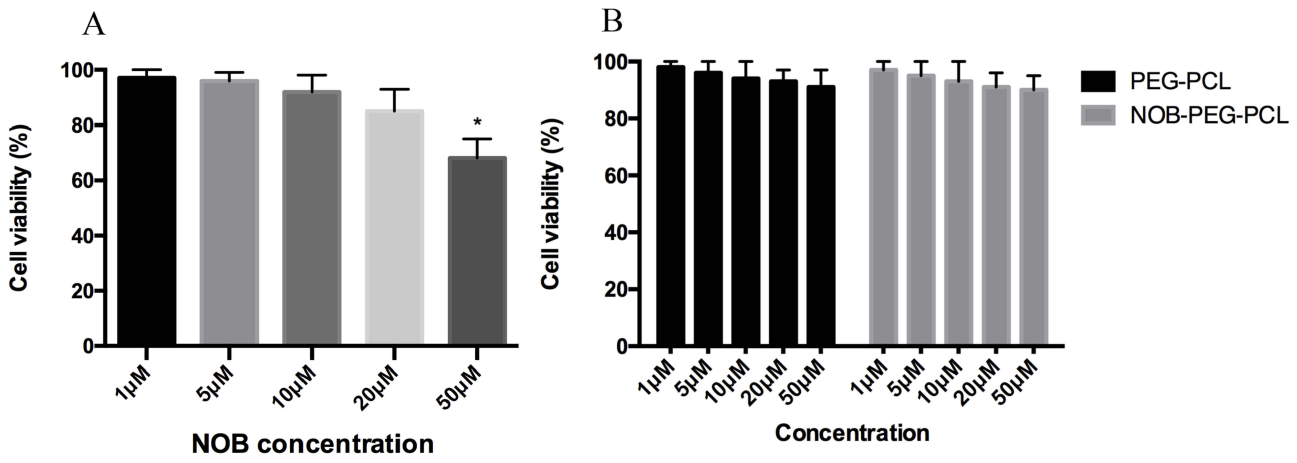


**Figure 3** In vitro study of NOB and NOB-loaded micelles by CCK-8 assay. (**A**) Viability of BMMs after exposure to NOB with different concentrations. (**B**) Viability of BMMs after exposure to PEG-PCL (dose: 1, 5, 10, 20, 50 μM) and NOB-PEG-PCL (dose: containing NOB 1, 5, 10, 20, 50 μM). *Represents $p<0.05$ compared with the untreated BMMs.

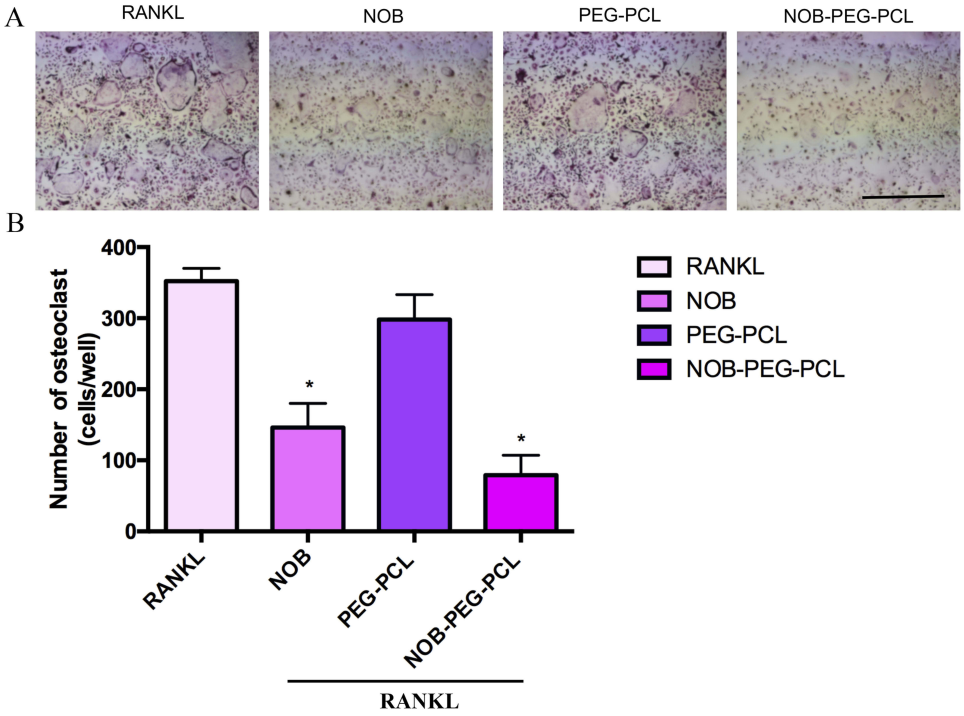


**Figure 4** (**A**) The effect of NOB, PEG-PCL, NOB-PEG-PCL on RANKL-induced OC formation. BMMs were prepared and incubated with NOB (dose: 50 μM) and PEG-PCL, NOB-PEG-PCL (dose: containing NOB 50 μM) in the presence of M-CSF (30 ng/mL) and RANKL (100 ng/mL). After 5 days, cells were fixed and stained for TRAP, and photographed. (**B**) The number of TRAP-positive osteoclasts per well was scored. *Represents $p<0.05$ compared with vehicle. The number of TRAP-positive multinucleated cells containing 3 or more nuclei was counted. Bar =1 mm. Data are expressed as the mean ± S.E.M.

50 μM) obviously decreased the amount of multi-nuclear TRAP-positive cells. Figure 4B shows that NOB and NOB-PEG-PCL inhibited the formation of $TRAP^+$ osteoclasts to 41% and 22% compared with control, respectively. These cells were characterized with morphological and biochemical markers for osteoclastogenesis. However, there was no significant difference between control cells and PEG-PCL group. Figure 5A shows that RANKL-stimulated cells expressed boosted TRAP activity. Prior to RANKL exposure, TRAP activity was suppressed by 37% ($P<0.05$) in NOB treatment and 55% ($P<0.05$) in NOB-PEG-PCL treatment. However, the NOB treatment may affect OC formation partly owing to cytotoxicity at the 50 μM concentration. The NOB-PEG-PCL treatment affecting OC

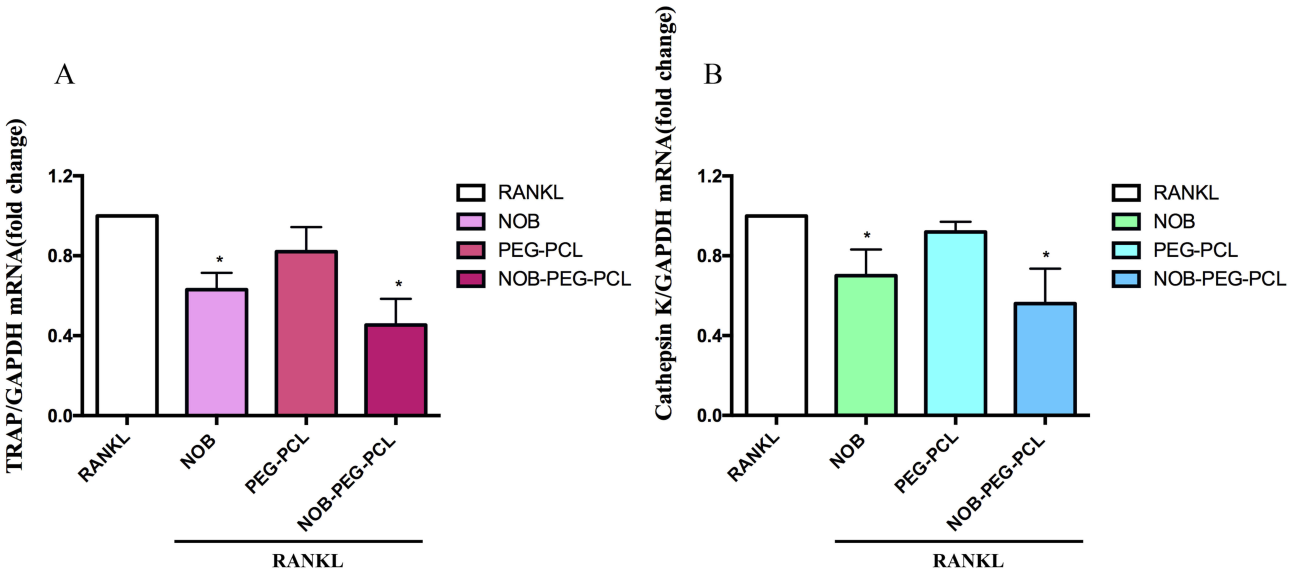


**Figure 5** (**A–B**) BMMs were prepared and incubated with NOB (dose: 50 μM) and PEG-PCL, NOB-PEG-PCL (dose: containing NOB 50 μM) in the presence of M-CSF (30 ng/mL) and RANKL (100 ng/mL). After 5 days, total RNA was isolated and subjected to qPCR analysis for TRAP and cathepsin K. The expression level stimulated by RANKL treatment was set at 1. *$p$<0.05 compared with vehicle.

formation was not due to cytotoxicity. Accord with this result, prior to RANKL exposure, cathepsin K was suppressed by 30% ($P$<0.05) in NOB treatment and 44% ($P$<0.05) in NOB-PEG-PCL treatment. In the presence of NOB-PEG-PCL and NOB, both TRAP and cathepsin K were obviously decreased after RANKL stimulation of OC (Figure 5B). In particular, NOB-PEG-PCL showed the lowest mRNA expressions for TRAP, cathepsin K in comparison to NOB treatment. These results suggested that NOB-PEG-PCL inhibit OC differentiation obviously. It is reported that Nobiletin is the main part in peels of some citrus fruits which could significantly suppress osteoporosis, skin inflammation, cancer, and cell proliferation.[40–42] However, NOB alone is cytotoxic at high concentrations unlike NOB-PEG-PCL which can be useful as a cytocompatible agent against osteoporosis.

Then, whether NOB-PEG-PCL affect the activation of mitogen-activated protein kinases (MAPK) signaling pathway was examined. RANKL binding to RANK activates MAPK and Akt. There are some reports that have shown that osteoclast differentiation is closely related with the activation of MAPKs (ERK1/2, p38, JNK1/2).[43] We used specific antibodies which can be bonded with each phosphorylated active form of RANKL-induced activation of MAPKs to detect the influence of NOB-PEG-PCL by Western blotting. After RANKL treatment for 30 mins, there was no obvious difference in the levels of non-phosphorylated inactive MAPKs but there exists in activation of ERK1/2, JNK1/2, and p38 MAPK (Figure 6). NOB and NOB-PEG-PCL significantly decreased the activation of these 3 MAPKs containing NOB 50 μM, whereas PEG-PCL treatment barely reduced the activation of these 3 MAPKs. Therefore, NOB-PEG-PCL system could suppress

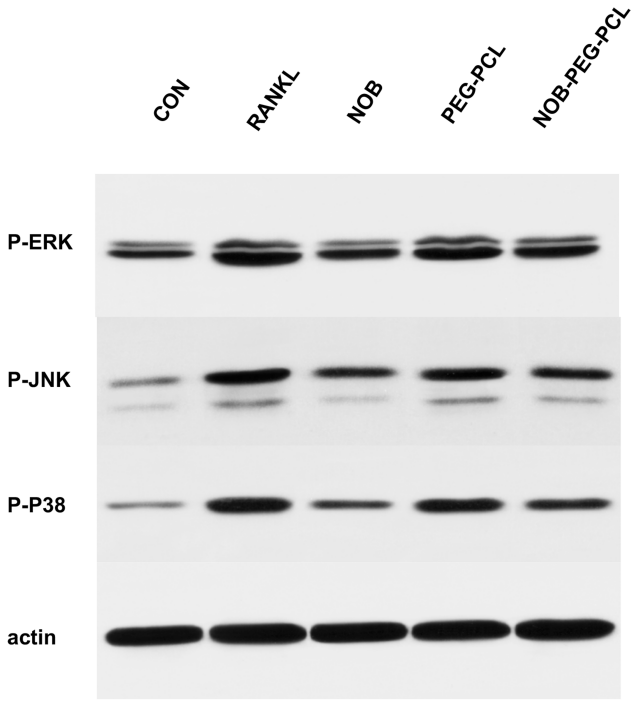


**Figure 6** Cytokine- and serum-starved BMM were exposed to RANKL (100 ng/mL). Phosphorylated forms of p38, ERK, JNK, and $\beta$-actin were detected by Western blots.

RANKL-induced osteoclastogenesis by inhibition of MAPKs signaling pathway which are important for osteoclastogenesis in OC formation.

## Anti-osteoporosis of NOB-PEG-PCL micelles

The quantitative analysis of the bone microstructural was used to investigate the influence of NOB-PEG-PCL vehicles on bone mass in vivo by using micro-CT (Figure 7A and B). In this study, osteoporotic mice were operated by ovariectomy treatment. Compared with the sham group, the BMD, BV/TV was notably reduced, and substantially increased Tb.Sp in OVX mice. Treatment with NOB or NOB-PEG-PCL (dose: NOB 50 μM) improved the reduced bone mass in OVX mice, while PEG-PCL group did not exhibit restoring ability compared with NOB-PEG-PCL due to lack of NOB against estrogen deficiency. More importantly, morphometric analysis showed that BV/TV in NOB-PEG-PCL group was notably greater and Tb.Sp was notably inferior than that in NOB group. Moreover, BMD in NOB-PEG-PCL group was demonstrated to be greater compared with the NOB group. Furthermore, there was no significant difference between NOB-PEG-PCL and NOB groups. Although we cannot distinguish osteoclasts in these histological sections (Figure 7C), it was visually observed that all ovariectomized groups had a higher amount of adipose tissue as compared to the sham group. OVX group had the most adipose tissue and NOB-PEG-PCL group had relatively less adipose tissue in all ovariectomized groups. The more adipose tissue, the less trabecular bone in all groups. Therefore, the trabecular bone is much more prominent in NOB-PEG-PCL group consistent with CT results. Hence, NOB loaded on the PEG-PCL micelles increased the ability of NOB against trabecular bone loss in OVX mode. Due to the inhibition of osteoclast formation expression of NOB, the reduced bone resorption in vivo may be induced by the sustained release of NOB when it is encapsulated in PEG-PCL micelles. Due to the enhanced effect of NOB on osteoclast formation and bone resorption,

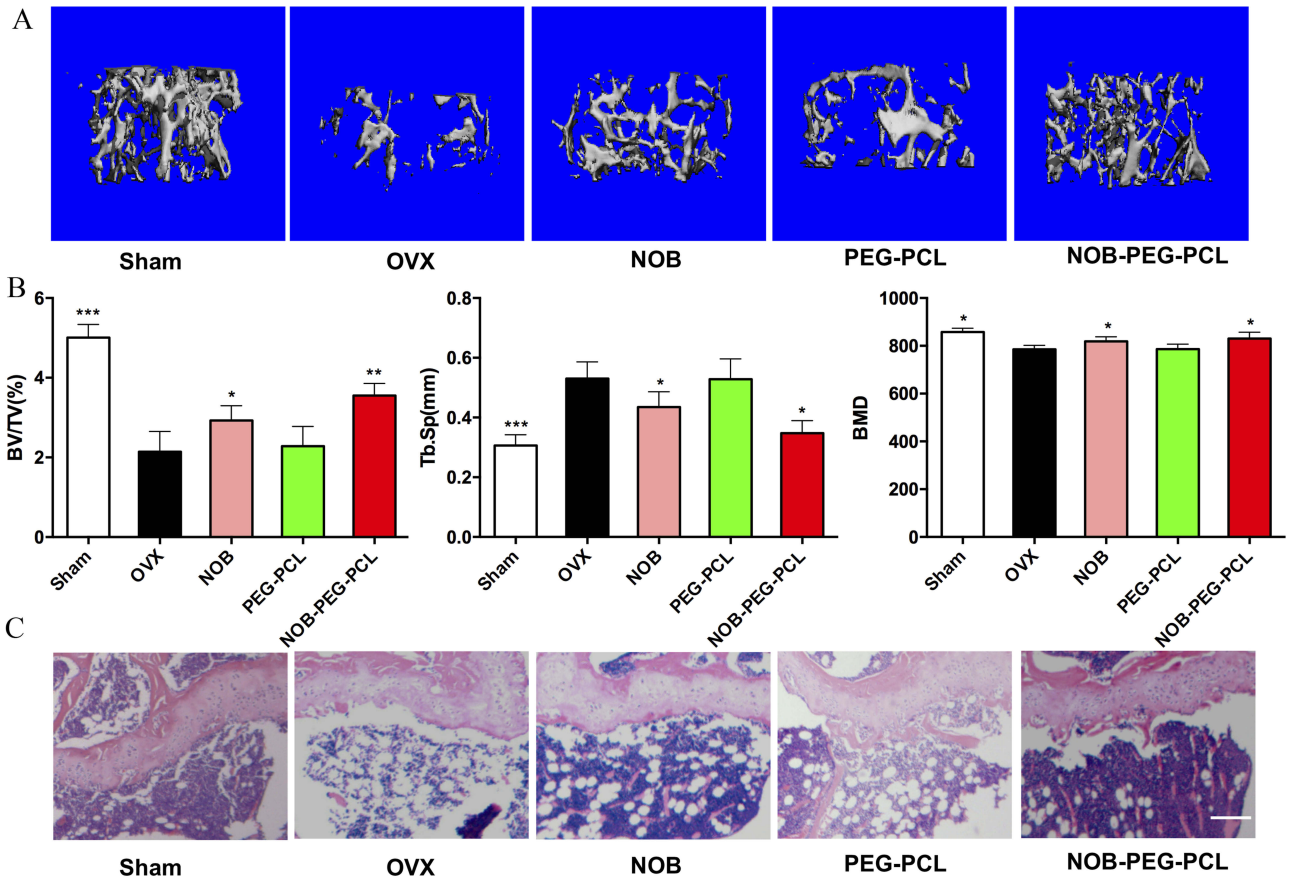


**Figure 7** Anti-osteoporosis of NOB-PEG-PCL micelles. (**A**) 3D image of the same position of femur head in the bone of sham, OVX, NOB, PEG-PCL, and NOB-PEG-PCL groups. Bar =1 mm. (**B**) bone volume/tissue volume (BV/TV), trabecular space (Tb.Sp), and bone mineral density (BMD) in the bone of sham, OVX, NOB, PEG-PCL, and NOB-PEG-PCL groups after 8 weeks treatment (mean ± SD). *Represents $p<0.05$ compared with OVX group. **Represents $P<0.01$ compared with OVX group. ***Represents $p<0.001$ compared with OVX group. (**C**) Histological analysis of femur from all experimental groups. Bar =100 μm.

NOB-PEG-PCL was demonstrated to achieve a better treatment effect in OVX model. It is suggested that NOB-PEG-PCL micelles fabricated in the present study could be applied as a novel therapeutic formula for managing osteoporosis.

## Conclusion

In this study, we successfully devised and made a new amphiphilic NOB-PEG-PCL beneficial vehicle on behalf of preventing and handling osteoporosis. The NOB-PEG-PCL repressed the RANKL-induced MAPK signaling pathway to finally inhibit the OC differentiation of BMMs. Moreover, the NOB-PEG-PCL micelles demonstrated good biocompatibility compared with NOB at high concentrations. Furthermore, NOB-PEG-PCL treatment prevented the bone loss induced by OVX. Overall, this NOB-loaded delivery system could be beneficially as remedial vehicles for treating osteoclast-related diseases of bone disorders and may have the potential to be applications in managing osteoporosis.

## Acknowledgment

We acknowledge the financial support from National Natural Science Foundation of China (81873715 and 81572114), the Innovation Program of Shanghai Municipal Education Commission (17140903600).

## Disclosure

The authors report no conflicts of interest in this work.

## References

1. Oftadeh R, Perez-Viloria M, Villa-Camacho JC, Vaziri A, Nazarian A. Biomechanics and mechanobiology of trabecular bone: a review. *J Biomech Eng*. 2015;137(1):010802. doi:10.1115/1.4029176
2. Paiva KBS, Granjeiro JM. Matrix metalloproteinases in bone resorption, remodeling, and repair. *Prog Mol Biol Transl Sci*. 2017;148:203–303.
3. Bandeira L, Lewiecki EM, Bilezikian JP. Romosozumab for the treatment of osteoporosis. *Expert Opin Biol Ther*. 2017;17(2):255–263.
4. Meeta RAA, Agashe SV, Wajahat A, Sarada CV, Vaidya AD, Vaidya RA. A clinical study of a standardized extract of leaves of Dalbergia sissoo (Roxb ex DC) in postmenopausal osteoporosis. *J Midlife Health*. 2019;10(1):37–42.
5. Dou C, Ding N, Zhao C, et al. Estrogen deficiency-mediated M2 macrophage osteoclastogenesis contributes to M1/M2 ratio alteration in ovariectomized osteoporotic mice. *J Bone Miner Res*. 2018;33(5):899–908.
6. Du Z, Xiao Y, Hashimi S, Hamlet SM, Ivanovski S. The effects of implant topography on osseointegration under estrogen deficiency induced osteoporotic conditions: histomorphometric, transcriptional and ultrastructural analysis. *Acta Biomater*. 2016;42:351–363.
7. Sharma D, Larriera AI, Palacio-Mancheno PE, et al. The effects of estrogen deficiency on cortical bone microporosity and mineralization. *Bone*. 2018;110:1–10.
8. Cai M, Yang L, Zhang S, Liu J, Sun Y, Wang X. A bone-resorption surface-targeting nanoparticle to deliver anti-miR214 for osteoporosis therapy. *Int J Nanomedicine*. 2017;12:7469–7482.
9. Offermanns V, Andersen OZ, Riede G, et al. Bone regenerating effect of surface-functionalized titanium implants with sustained-release characteristics of strontium in ovariectomized rats. *Int J Nanomedicine*. 2016;11:2431–2442.
10. Teitelbaum SL. Bone resorption by osteoclasts. *Science*. 2000;289(5484):1504–1508. doi:10.1126/science.289.5484.1504
11. Bar-Shavit Z. The osteoclast: a multinucleated, hematopoietic-origin, bone-resorbing osteoimmune cell. *J Cell Biochem*. 2007;102(5):1130–1139. doi:10.1002/jcb.21553
12. Boyce BF. Advances in the regulation of osteoclasts and osteoclast functions. *J Dent Res*. 2013;92(10):860–867. doi:10.1177/0022034513500306
13. Kylmaoja E, Nakamura M, Tuukkanen J. Osteoclasts and remodeling based bone formation. *Curr Stem Cell Res Ther*. 2016;11(8):626–633.
14. De Vries TJ, Schoenmaker T, Aerts D, et al. M-CSF priming of osteoclast precursors can cause osteoclastogenesis-insensitivity, which can be prevented and overcome on bone. *J Cell Physiol*. 2015;230(1):210–225. doi:10.1002/jcp.24702
15. Yamaguchi T, Movila A, Kataoka S, et al. Proinflammatory M1 macrophages inhibit RANKL-induced osteoclastogenesis. *Infect Immun*. 2016;84(10):2802–2812. doi:10.1128/IAI.00461-16
16. Joo JH, Huh JE, Lee JH, et al. A novel pyrazole derivative protects from ovariectomy-induced osteoporosis through the inhibition of NADPH oxidase. *Sci Rep*. 2016;6:22389. doi:10.1038/srep22389
17. Xia G, Wang X, Sun H, Qin Y, Fu M. Carnosic acid (CA) attenuates collagen-induced arthritis in db/db mice via inflammation suppression by regulating ROS-dependent p38 pathway. *Free Radic Biol Med*. 2017;108:418–432. doi:10.1016/j.freeradbiomed.2017.03.023
18. Panteghini M, Pagani F. Reference intervals for two bone-derived enzyme activities in serum: bone isoenzyme of alkaline phosphatase (ALP) and tartrate-resistant acid phosphatase (TR-ACP). *Clin Chem*. 1989;35(1):180–181.
19. Kyllonen L, D'Este M, Alini M, Eglin D. Local drug delivery for enhancing fracture healing in osteoporotic bone. *Acta Biomater*. 2015;11:412–434.
20. Lone J, Parray HA, Yun JW. Nobiletin induces brown adipocyte-like phenotype and ameliorates stress in 3T3-L1 adipocytes. *Biochimie*. 2018;146:97–104.
21. Sp N, Kang DY, Joung YH, et al. Nobiletin inhibits angiogenesis by regulating Src/FAK/STAT3-mediated signaling through PXN in ER (+) breast cancer cells. *Int J Mol Sci*. 2017;18(5):935.
22. Aoki K, Yokosuka A, Mimaki Y, Fukunaga K, Yamakuni T. Nobiletin induces inhibitions of Ras activity and mitogen-activated protein kinase kinase/extracellular signal-regulated kinase signaling to suppress cell proliferation in C6 rat glioma cells. *Biol Pharm Bull*. 2013;36(4):540–547.
23. Kanda K, Nishi K, Kadota A, Nishimoto S, Liu MC, Sugahara T. Nobiletin suppresses adipocyte differentiation of 3T3-L1 cells by an insulin and IBMX mixture induction. *Biochim Biophys Acta*. 2012;1820(4):461–468.
24. Harada S, Tominari T, Matsumoto C, et al. Nobiletin, a polymethoxy flavonoid, suppresses bone resorption by inhibiting NFkappaB-dependent prostaglandin E synthesis in osteoblasts and prevents bone loss due to estrogen deficiency. *J Pharmacol Sci*. 2011;115(1):89–93.
25. Khachane P, Date AA, Nagarsenker MS. Eudragit EPO nanoparticles: application in improving therapeutic efficacy and reducing ulcerogenicity of meloxicam on oral administration. *J Biomed Nanotechnol*. 2011;7(4):590–597.
26. Gagliardi M, Bardi G, Bifone A. Polymeric nanocarriers for controlled and enhanced delivery of therapeutic agents to the CNS. *Ther Deliv*. 2012;3(7):875–887.
27. Dudhipala N, Veerabrahma K. Candesartan cilexetil loaded nanodelivery systems for improved oral bioavailability. *Ther Deliv*. 2017;8(2):79–88.

28. Zhang Y, He L, Yue S, Huang Q, Zhang Y, Yang J. Characterization and evaluation of a self-microemulsifying drug delivery system containing tectorigenin, an isoflavone with low aqueous solubility and poor permeability. *Drug Deliv*. 2017;24(1):632–640.
29. e Silva C, de Oliveira D, Estevanato LL, et al. Successful strategy for targeting the central nervous system using magnetic albumin nanospheres. *J Biomed Nanotechnol*. 2012;8(1):182–189.
30. Kesharwani SS, Kaur S, Tummala H, Sangamwar AT. Overcoming multiple drug resistance in cancer using polymeric micelles. *Expert Opin Drug Deliv*. 2018;15(11):1127–1142.
31. Kesharwani SS, Kaur S, Tummala H, Sangamwar AT. Multifunctional approaches utilizing polymeric micelles to circumvent multidrug resistant tumors. *Colloids Surf B Biointerfaces*. 2019;173:581–590.
32. Lei Y, Xu Z, Ke Q, et al. Strontium hydroxyapatite/chitosan nanohybrid scaffolds with enhanced osteoinductivity for bone tissue engineering. *Mater Sci Eng C Mater Biol Appl*. 2017;72:134–142.
33. Zhu C, Xiao J, Tang M, Feng H, Chen W, Du M. Platinum covalent shell cross-linked micelles designed to deliver doxorubicin for synergistic combination cancer therapy. *Int J Nanomedicine*. 2017;12:3697–3710.
34. Shan F, Liu Y, Jiang H, Tong F. In vitro and in vivo protein release and anti-ischemia/reperfusion injury properties of bone morphogenetic protein-2-loaded glycyrrhetinic acid-poly(ethylene glycol)-b-poly(l-lysine) nanoparticles. *Int J Nanomedicine*. 2017;12:7613–7625.
35. Oliveira MC, Di Ceglie I, Arntz OJ, et al. Milk-derived nanoparticle fraction promotes the formation of small osteoclasts but reduces bone resorption. *J Cell Physiol*. 2017;232(1):225–233.
36. Grossen P, Witzigmann D, Sieber S, Huwyler J. PEG-PCL-based nanomedicines: a biodegradable drug delivery system and its application. *J Control Release*. 2017;260:46–60.
37. Hu J, Zeng F, Wei J, Chen Y, Chen Y. Novel controlled drug delivery system for multiple drugs based on electrospun nanofibers containing nanomicelles. *J Biomater Sci Polym Ed*. 2014;25(3):257–268.
38. Yao W, Xu P, Pang Z, et al. Local delivery of minocycline-loaded PEG-PLA nanoparticles for the enhanced treatment of periodontitis in dogs. *Int J Nanomedicine*. 2014;9:3963–3970.
39. Gong CY, Wu QJ, Dong PW, et al. Acute toxicity evaluation of biodegradable in situ gel-forming controlled drug delivery system based on thermosensitive PEG-PCL-PEG hydrogel. *J Biomed Mater Res B*. 2009;91(1):26–36.
40. Moon JY, Cho SK. Nobiletin induces protective autophagy accompanied by ER-stress mediated apoptosis in human gastric cancer SNU-16 cells. *Molecules*. 2016;21(7):914.
41. Murakami A, Nakamura Y, Torikai K, et al. Inhibitory effect of citrus nobiletin on phorbol ester-induced skin inflammation, oxidative stress, and tumor promotion in mice. *Cancer Res*. 2000;60(18):5059–5066.
42. Murakami A, Song M, Katsumata S, Uehara M, Suzuki K, Ohigashi H. Citrus nobiletin suppresses bone loss in ovariectomized ddY mice and collagen-induced arthritis in DBA/1J mice: possible involvement of receptor activator of NF-kappaB ligand (RANKL)-induced osteoclastogenesis regulation. *Biofactors*. 2007;30(3):179–192.
43. Zhang Y, Wang Z, Xie X, et al. Tatarinan N inhibits osteoclast differentiation through attenuating NF-kappaB, MAPKs and Ca(2+)-dependent signaling. *Int Immunopharmacol*. 2018;65:199–211.